X-523-70-207
PREPRINT

NASA TM X- 63958

DATA FILTERING FOR THE NEW MINITRACK SYSTEM

V. R. SIMAS
D. E. SANTARPIA

MAY 1970

GSFC
GODDARD SPACE FLIGHT CENTER
GREENBELT, MARYLAND

X-523-70-207

DATA FILTERING FOR THE NEW MINITRACK SYSTEM

V. R. Simas

D. E. Santarpia

May 1970

Goddard Space Flight Center
Greenbelt, Maryland

PRECEDING PAGE BLANK NOT FILMED.

CONTENTS

PRECEDING PAGE BLANK NOT FILMED.

DATA FILTERING FOR THE NEW MINITRACK SYSTEM

V. R. Simas

D. E. Santarpia

ABSTRACT

Narrowband predetection filtering is required to avoid deterioration in the SNR by the signal detector. The minimum passband, set by Doppler and other frequency uncertainties, is 7 KHz. Electronic post-detection filtering and data smoothing by polynomial fitting are equivalent, providing sufficient data samples are supplied. Since the data smoothing process exhibits an effect on the data equivalent to a filter having a passband of a fraction of a Hz, the electronic filter does not control the phase uncertainties. The proper data sampling rate is directly proportional to the post-detection bandwidth, B_n. Because of this factor, B_n should be made small avoiding excessive costs in relaying the data to GSFC and processing the data in the orbit determination sequence. Passive filters for B_n cannot function without introducing phase delays in the data very much greater than the desired accuracy of the system. For this reason, the tracking filter is selected which can follow, with a negligible error, the first, second and third derivatives of the signal phase resulting from a worst case spacecraft pass of 100 miles altitude directly over the station. The loop bandwidth, B_L, of this filter is a compromise between sampling rate and loop acquisition time. The best value is considered to be 5 Hz which provides an acquisition time of 0.8 seconds and a sampling rate of 5 s/sec.

DATA FILTERING FOR THE NEW MINITRACK SYSTEM

Introduction

There are some interesting features in the signal filtering that occur in the Minitrack system. The three types of filtering that directly effect system performance are the pre-detection passband, the post-detection passband and finally the smoothing and polynomial fitting [1] that is accomplished on the data by the computers at GSFC.

The pre-detection filtering, although related to the other two, can be discussed independently. Its function is to reduce the noise on the signal that is subsequently demodulated by either an envelope or a square law detector. As the pre-detected signal-to-noise ratio (SNR) descends to unity and below for a non-coherent detector of this type, the SNR output of the detector becomes increasingly degraded. Thus, it is desired that the predetection filter be as narrow as possible. The width of this filter, however, must be sufficient to encompass the Minitrack beacon signal in the presence of doppler and other frequency uncertainties. For the Minitrack parameters at 136 MHz, it can be shown that at least a 7 KHz passband is required. The present Minitrack utilizes a 10 KHz linear phase filter.

Post-detection electronic filtering and data smoothing are highly interrelated. From a theoretical viewpoint, it can be said that there is no necessity for electronic filtering because the smoothing operation which follows is in essence a filter with a very narrow passband, thereby precluding any effect the electronic filter has on the data. Practical considerations, however, warrant judicious selection of the electronic filtering characteristics for several reasons: (1) Phase readings are ambiguous in that they repeat every 360 degrees, thus, large phase fluctuations would introduce errors in the data in excess of the errors produced in quantizing the data, and would therefore require substantially more complexity and expense in the data smoothing process, (2) Lightly filtered, thus noisy data, requires substantially higher sampling rates for signal processing, thereby increasing the expense of transmitting this data from the field stations to GSFC, (3) The cost of processing this lengthy stream of data by the orbit determination computers would be unjustifiably excessive.

The extent of the electronic filtering is a compromise between the factors mentioned above and the errors and operational complications introduced by

the filter. The existing Minitrack utilizes a passive filter with a passband of 10 Hz for the fine baseline data. For perigee passes, where the spacecraft altitude is approximately 100 miles, the rate of change in phase output of the interferometer, $\dot{\Phi}$, is on the order of 2.5 Hz or 900 degrees per second. Assuming the single tuned, 10 Hz wide, Minitrack Filter is tuned precisely to the difference frequency, a change in frequency, Δf, of 2.5 Hz causes close to 25 degrees of phase shift through this filter. This is a factor of about 75 times greater than the resolution of the system and produces an intolerable error even though the data is compensated for in the data processing sequences. If a passive filter were the only solution to this problem, then it would probably be better to widen it substantially beyond the existing 10 Hz passband even though the sampling rate would increase materially. A phase-lock-loop tracking filter, because of its capability of providing narrowband filtering with vastly reduced phase shifts or time delay errors, appears to offer an ideal solution to this problem, assuming of course, that its characteristics are properly matched to the Minitrack signals.

Phase-Lock-Loop Tracking Filter

There is an apparent contradiction involved with the operation of tracking filters. Certain types of digital filters store data and can therefore look into the future as well as the past for their averaging functions thereby eliminating, for linear functions at least, time delay errors. These devices can, within limits, smooth out the noise fluctuations with no delay between the smoothed data and the applied data. Tracking filters achieve the same results in real time. From the viewpoint of standard filter theory, this appears most incongruous, since conventional real time filtering is always involved with averaging past data so that the smoothed data is delayed by an amount corresponding to the filter weighting function. This is true even for data which changes linearly. An interpretation as to how the tracking filter accomplishes this feat can best be understood from an examination of Figure 1. The block diagram shows an idealized third order tracking filter in which the voltage controlled oscillator (VCO) is replaced by an integrator, a voltage controlled phase shifter(VCϕ), and an oscillator. This manner of drawing the diagram portrays the integration that occurs due to the phase output of a VCO being the integral of the controlled frequency. We can now examine the operation of the circuit by applying waveforms to the loop ϕ detector and deducing the relationship between the voltage analog of the phase variations of the applied signal and the VCO signal which is also the signal output from this filter.

Consider applications of functions of increasing order to the loop. The first input is simply a phase offset. If the final integrator output, $V_d(\phi)$, is the proper voltage offset, the phase shift through the VCϕ will be sufficient to make

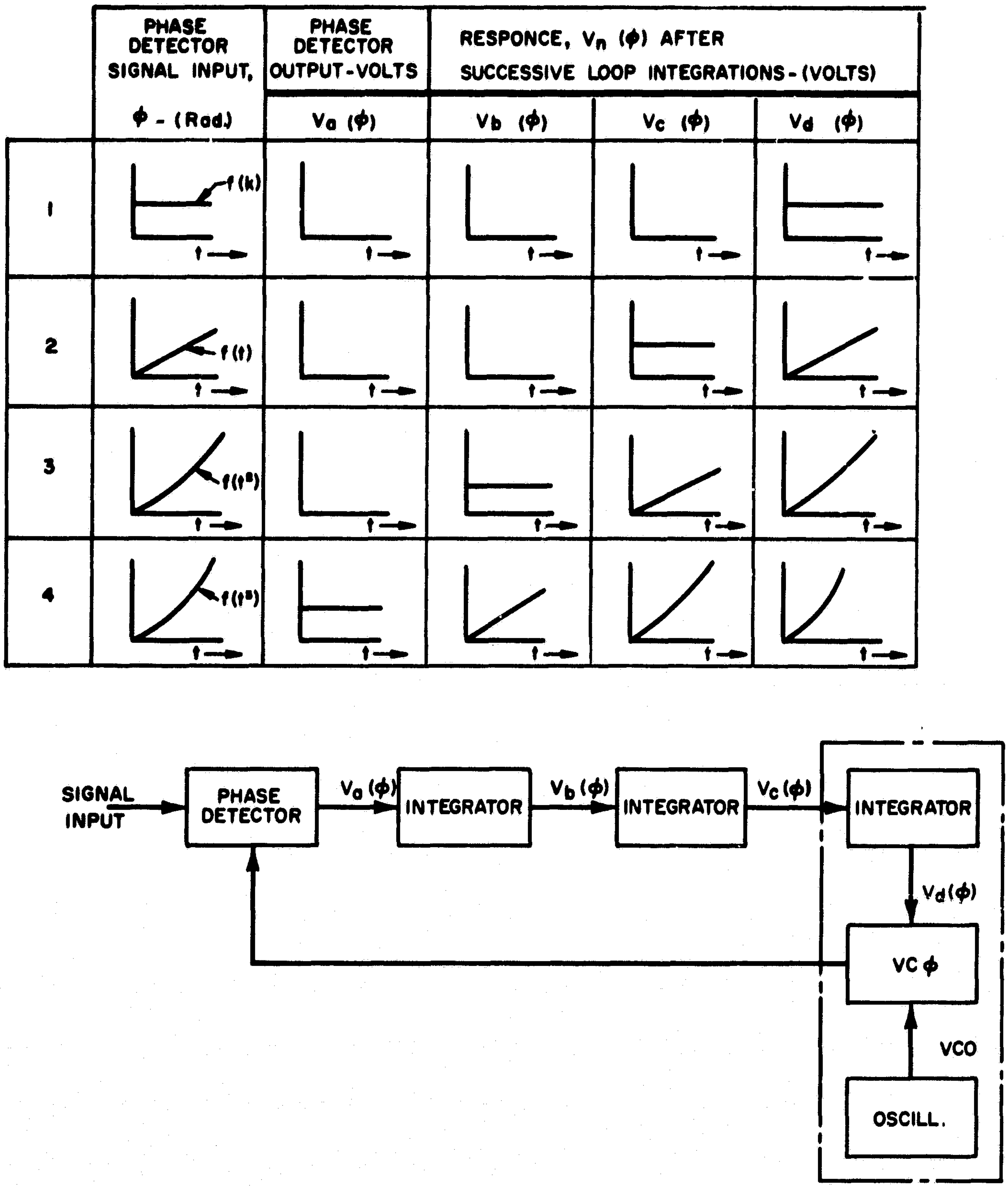
PHASE DETECTOR SIGNAL INPUT, ϕ - (Rad.)
PHASE DETECTOR OUTPUT-VOLTS
RESPONCE, V_n (ϕ) AFTER SUCCESSIVE LOOP INTEGRATIONS-(VOLTS)
V_a (ϕ)
V_b (ϕ)
V_c (ϕ)
V_d (ϕ)
1
2
3
4
f (k)
f (t)
f (t^2)
f (t^3)
t
SIGNAL INPUT
PHASE DETECTOR
INTEGRATOR
INTEGRATOR
INTEGRATOR
VC ϕ
VCO
OSCILL.

Figure 1

the tracking filter output (VCϕ output) signal coincident and identical to the tracking filter signal input. To achieve this voltage offset, the input to the last integrator $V_c(\phi)$, will require zero voltage, and likewise for voltages $V_b(\phi)$ and $V_a(\phi)$, If they are not at the proper level, $V_d(\phi)$ will be a voltage of higher order than that required to make the tracking filter output a replica of the signal input. The second row of waveforms shows a ramp change in phase applied to the tracking filter. In the same manner as before the waveform, $V_d(\phi)$ must be a ramp change in voltage. This can be maintained by a voltage offset $V_c(\phi)$. The voltages $V_b(\phi)$ and $V_a(\phi)$ are zero to maintain a zero difference between input and output. The third row of waveforms shows a quadratic change in applied phase. In the same manner as above, the output of the phase detector, $V_a(\phi)$, can now be zero. Finally for cubic changes in applied phase, the phase detector must produce a constant offset voltage, $V_a(\phi)$ whose magnitude is dependent upon the loop gain. Only for this last case is there a phase difference, hence a time offset, between the signal input and tracking filter output, this difference corresponding to the voltage offset at the output of the phase detector.

It is important to realize that the deductions discussed above are predicated on steady state conditions only; that is, if a quadratic change in phase is assumed, then it has been changing a sufficient period, according to a quadratic relationship, for transient voltages in the loop to have asymptotically decayed to zero or to a steady state value. It is also important to note that a signal input can be highly filtered in this tracking filter with no phase or time delay, providing changes in applied phase (or frequency) occur sufficiently smoothly that third order terms and higher are negligible.

As further evidence, let us view the effect that an artificial loop time delay would have on the difference between output and input. Consider, for example, the second row of waveforms where the applied signal contains a ramp change in phase. If a loop time delay were introduced after the last integrator it would appear at first glance that a change in phase would occur between the signal input and tracking loop output since the ramp voltage fed back to the VCO would be delayed. The fact is, however, the voltage, $V_d(\phi)$, after the transient has decayed, will vary (after the delay) to reduce the phase difference between the signal input and the tracking filter output to zero. Thus, the circuit even in the case of artificially induced loop delays produces control voltages which can be considered to anticipate the proper value occuring in the future. This set of circumstances becomes plausible when considering the nature of the loop input signals. Since we are considering only well-defined waveforms in steady state, the loop has a priori knowledge and will track, without phase lags, waveforms which can be described by equations whose order is one less than the number of loop integrators. For phase fluctuations of no higher order than

quadratic, our idealized filter, will anticipate perfectly the future sequence of events and will compensate accordingly.

Because of the unique properties of tracking filters, as discussed above, such a device appears to be most appropriate for the Minitrack post-detection filter where it is desired that narrow band filtering be accomplished with negligible phase delay.

Another source of phase error which a tracking filter must accommodate is the dynamic phase error introduced by the time derivatives of the phase output of the Minitrack interferometer system, Φ. These time derivatives are functions of spacecraft-earth station geometry and spacecraft dynamics. It is important, therefore, to determine the maximum total phase error possible due to a severe satellite tracking situation and the tracking filter bandwidth required to maintain a phase error tolerance of, say, one count or .36°.

Tracking Dynamic Phase Errors

Consider a worst case dynamic tracking situation in which a spacecraft orbiting at 5 mi/sec passes overhead in a 100 mile high circular orbit. Referring to Figure 2:

r = earth radius = 4,000 miles
h = orbit height = 100 miles
R = $r + h$
V_t = spacecraft tangential velocity (5 miles/sec) = $R\omega = -R\dot{\alpha}$
α, θ, β = are geometric angles determined by the spacecraft, station and earth in radians.

From the geometry of Figure 1:

$$\beta = 90 - \alpha - \theta$$

and (1)

$$\dot{\beta} = -\dot{\alpha} - \dot{\theta}$$

but

$$\dot{\alpha} = -\frac{V_t}{R} \tag{2}$$

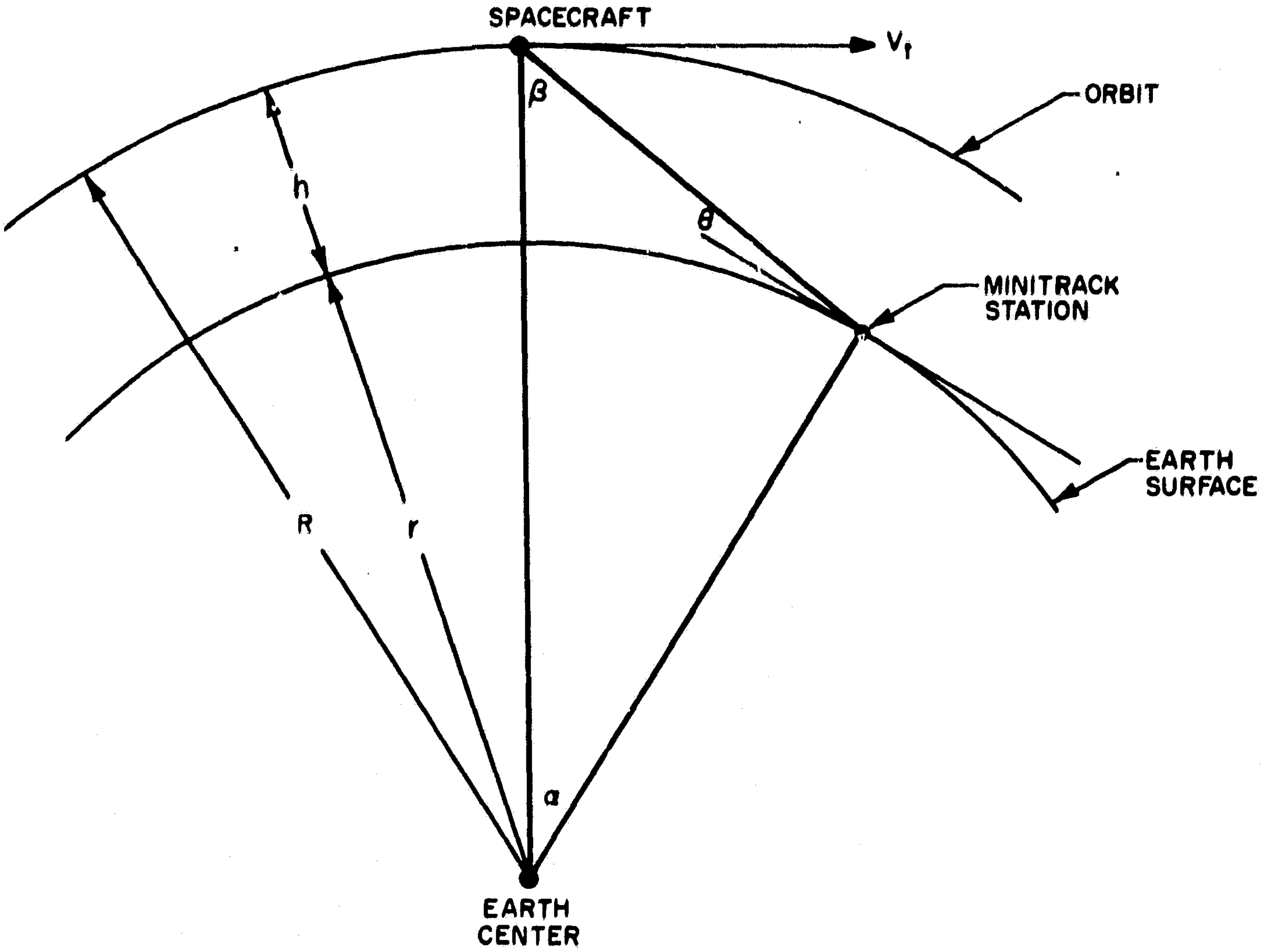

Figure 2

Substituting equation (2) into (1):

$$\dot{\beta} = + \frac{V_t}{R} - \dot{\theta} \tag{3}$$

also

$$\beta = \sin^{-1}\left(\frac{r}{R}\cos\theta\right)$$

and

$$\dot{\beta} = -\frac{r\dot{\theta}\sin\theta}{R\left(1-\frac{r^2}{R^2}\cos^2\theta\right)^{1/2}} \tag{4}$$

Equating (3) and (4) and solving for $\dot{\theta}$, we obtain:

$$\dot{\theta} = -\frac{\frac{V_t}{R}\left(1-\frac{r^2}{R^2}\cos^2\theta\right)^{1/2}}{\frac{r}{R}\sin\theta-\left(1-\frac{r^2}{R^2}\cos^2\theta\right)^{1/2}} \tag{5}$$

Taking the 2nd Derivative of (5):

$$\ddot{\theta} = -\frac{\left[\frac{r}{R}\sin\theta-\left(1-\frac{r^2}{R^2}\cos^3\theta\right)^{1/2}\right]\cdot\left[\frac{V_t}{2R}\left(1-\frac{r^2}{R^2}\cos^2\theta\right)^{-1/2}\right]\cdot\left[\frac{r^2}{R^2}\dot{\theta}\sin 2\theta\right]}{\left[\frac{r}{R}\sin\theta-\left(1-\frac{r^2}{R^2}\cos^2\theta\right)^{1/2}\right]^2}$$

$$+\frac{\left[\frac{V_t}{R}\left(1-\frac{r^2}{R^2}\cos^2\theta\right)^{1/2}\right]\left[\frac{r\dot{\theta}}{R}\cos\theta-\frac{1}{2}\left(1-\frac{r^2}{R^2}\cos^2\theta\right)^{-1/2}\left(\frac{r^2}{R^2}\dot{\theta}\sin 2\theta\right)\right]}{\left[\frac{r}{R}\sin\theta-\left(1-\frac{r^2}{R^2}\cos^2\theta\right)^{1/2}\right]^2} \tag{6}$$

From the interferometer relationship:[2]

$$\cos\theta = \frac{\Phi}{B}$$

where:

B = Minitrack interferometer baseline of 50 wavelengths

Φ = Phase output of the minitrack interferometer system in cycles.

but from Figure 1:

$$\cos \theta = \frac{R}{r} \sin \beta$$

therefore,

$$\Phi = \frac{BR}{r} \sin \beta$$

differentiating once and substituting equation 3 for $\dot{\beta}$:

$$\dot{\Phi} = + \frac{V_t B}{r} \cos \beta - \frac{\dot{\theta} BR}{r} \cos \beta \tag{7}$$

taking the second derivative:

$$\ddot{\Phi} = \frac{B\dot{\beta}}{r} \sin \beta (- V_t + R\dot{\theta}) - \frac{\ddot{\theta} BR}{r} \cos \beta \tag{8}$$

Substitution of equations (4), (5) and (6) into (8) gives the relationship of $\ddot{\Phi}$, the phase acceleration, to spacecraft-earth tangential angle, θ. A solution to equation (8) was obtained by computer for $0 \leq \theta \leq \pi$ in .01 radian increments.

In addition, computer differencing was used to determine the rate of change of phase acceleration, $\dddot{\Phi}$. A plot of $\ddot{\Phi}$ and $\dddot{\Phi}$ as a function of spacecraft-earth tangential angle, θ, is shown in Figure 3.

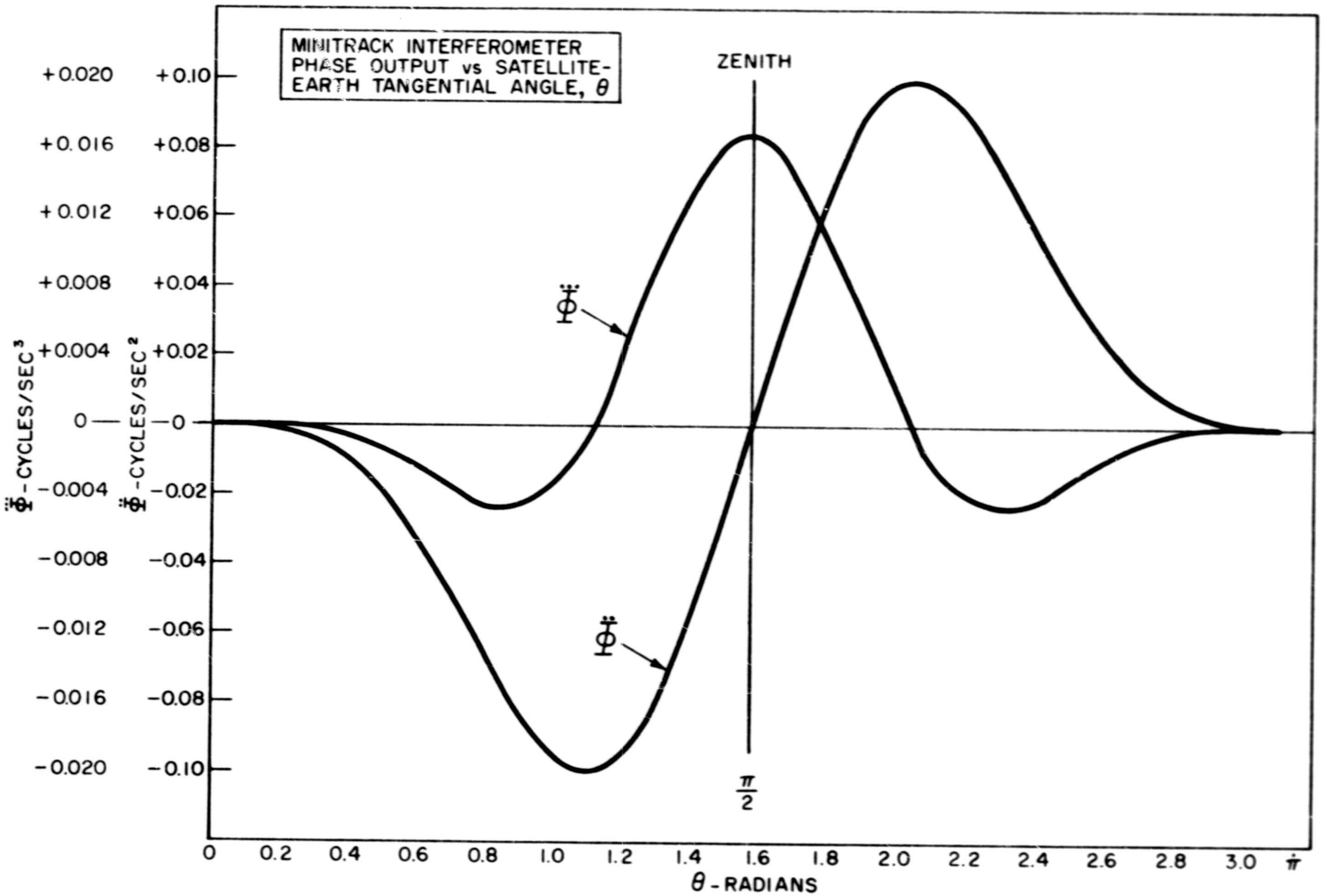
MINITRACK INTERFEROMETER PHASE OUTPUT vs SATELLITE-EARTH TANGENTIAL ANGLE, θ
ZENITH
$\dddot{\Phi}$
$\ddot{\Phi}$
$\dddot{\Phi}$ - CYCLES/SEC^3
$\ddot{\Phi}$ - CYCLES/SEC^2
+0.020
+0.016
+0.012
+0.008
+0.004
0
-0.004
-0.008
-0.012
-0.016
-0.020
+0.10
+0.08
+0.06
+0.04
+0.02
0
-0.02
-0.04
-0.06
-0.08
-0.10
0
0.2
0.4
0.6
0.8
1.0
1.2
1.4
1.6
1.8
2.0
2.2
2.4
2.6
2.8
3.0
π
$\frac{\pi}{2}$
θ - RADIANS

Figure 3

Determination of Phase-Lock-Loop Tracking Bandwidth

In a system such as the 136 MHz Minitrack, the steady state phase error, in radians, introduced in the tracking loop due to $\ddot{\Phi}$ and $\dddot{\Phi}$ is described by Reedy and Mallinkrodt[3] to be:

$$\epsilon(2^{nd}\text{ order}) \doteq \left| \frac{2\pi}{\omega_n^2}\ddot{\Phi} - \frac{2\sqrt{2}\,\pi}{\omega_n^3}\dddot{\Phi} \right| \tag{6}$$

$$\epsilon(3^{rd}\text{ order}) \doteq \left| -\frac{8\pi}{\omega_n^3}\dddot{\Phi} \right| \tag{7}$$

where $\ddot{\Phi}$, $\dddot{\Phi}$ are time derivatives of the interferometer phase difference (in cycles/sec^2 and cycles/sec^3 respectively) at the input to the loop phase detector, and ω_n is the "natural frequency" of the loop and is equated to the one sided noise bandwidth B_L, of the loop by[3,4]:

$$\omega_n(2^{nd}\text{ order}) = \frac{B_L}{.53} \quad \text{(for damping factor .707)}$$

$$\omega_n(3^{rd}\text{ order}) = \frac{B_L}{.73} \quad \text{(Mallinckrodt Loop)}$$

substituting this relationship for ω_n, we obtain:

$$\epsilon(2^{nd}\text{ order}) \doteq \left| \frac{1.77}{B_L^2}\ddot{\Phi} - \frac{1.33}{B_L^3}\dddot{\Phi} \right| \tag{8}$$

$$\epsilon(3^{rd}\text{ order}) \doteq \left| -\frac{9.78}{B_L^3}\dddot{\Phi} \right| \tag{9}$$

Maximum total steady state phase error for a second order tracking loop occurs for a spacecraft at ±27° off zenith. At this spatial position $\ddot{\Phi}$ is maximum and $\dddot{\Phi} = 0$. For a third order loop, the maximum phase error occurs at

zenith where $\dddot{\Phi}$ is maximum; hence equations (8) and (9) reduce to:

$$\epsilon_{max}(2^{nd}\ \text{order}) \doteq \left| \frac{1.77}{B_L^2} \ddot{\Phi}_{max} \right| \tag{10}$$

$$\epsilon_{max}(3^{rd}\ \text{order}) \doteq \left| -\frac{9.78}{B_L^3} \dddot{\Phi}_{max} \right| \tag{11}$$

solving for B_L, we obtain:

$$B_L(2^{nd}\ \text{order}) \doteq \left(\left| \frac{1.77}{\epsilon_{max}} \ddot{\Phi}_{max} \right| \right)^{1/2} \tag{12}$$

$$B_L(3^{rd}\ \text{order}) \doteq \left(\left| -\frac{9.78}{\epsilon_{max}} \dddot{\Phi}_{max} \right| \right)^{1/3} \tag{13}$$

The maximum values of $\ddot{\Phi}$ and $\dddot{\Phi}$ from Figure 3 are .0987 cycles/sec^2 and .0167 cycles/sec^3 respectively. Inserting these values in the above equations with ϵ_{max} set to 0.36 degrees (1 count) results in:

$$B_L\ (\text{2nd order}) = 5\ \text{Hz.}$$

$$B_L\ (\text{3rd order}) = 3\ \text{Hz.}$$

Having set a lower bound for selecting acceptable phase lock loop tracking filter bandwidths, it is necessary to examine the effect B_L has on data acquisition time and the subsequent smoothing operation performed by the GSFC orbit determination computer.

Acquisition Time and Data Smoothing

Acquisition time is a most important parameter in the selection of acceptable phase-lock-tracking filters. Since a 100 mile orbiting spacecraft is in the main lobe of the minitrack system, only 4 or 5 seconds the acquisition time should be on the order of 1 second. Assuming the interferometer system begins operation as a spacecraft just enters the main lobe, approximately 5° off zenith, the following phase error-producing interferometer phase derivatives exist:

$$\Phi = -.225 \text{ rad.}$$

$$\dot{\Phi} = 15.07 \frac{\text{rad.}}{\text{sec}}$$

$$\ddot{\Phi} = .1858 \frac{\text{rad.}}{\text{sec}^2}$$

$$\dddot{\Phi} = -.0992 \frac{\text{rad.}}{\text{sec}^3}$$

As the satellite approaches zenith, $\dot{\Phi}$ and $\dddot{\Phi}$ are increasing to a maximum value and $\ddot{\Phi}$ is decreasing to zero; however, at commencement of system operation, transient phase errors in the tracking filter are produced which require a finite time to decay to the desired steady state resolution of 0.36°. On the basis of the transient response of a 5 Hz second order phase lock loop whose dampening factor is $\sqrt{2/2}$, approximately 0.8 second is required to reduce tracking loop transient phase errors to .36°.

The transient response of a third order loop, given the same initial phase error producing parameters given above, is greater than four seconds[5] which is a large portion of the main lobe tracking time.

It is apparent that a 5 Hz second order loop will adequately meet the criteria set for acceptable acquisition time, while a 3 Hz third order loop will not. The third order bandwidth can be widened to reduce the loop transient error response time to less than a second at the expense of S/N ratio improvement and increased sampling rate. About 20 Hz would be required. It is also possible to attempt acquisition earlier in the pass, that is, prior to the main lobe beam width. If acquisition is attempted prior to the main lobe null, questions arise as to the magnitude of the phase errors introduced due to perturbations experienced in passing through the lobe nulls. Would these phase errors be of sufficient magnitude to produce a loss of lock? Would they be of sufficient magnitude to produce longer transient phase errors? For these reasons the 2nd order loop with a 5 Hz bandwidth is the most appropriate for our application.

The smoothing program performed at GSFC takes the total data message consisting of N data points and by a polynomial fitting process determines the spacecraft trajectory arc over which the data was observed. The uncertainty of the smoothed data sent to GSFC can be reduced by a factor very nearly equal

to $(1/N)^{1/2}$(6) (where N is the number of samples) providing the sampling rate is sufficiently low that the noise on these samples is uncorrelated. The noise starts to become correlated when the sampling rate is on the same order as the post detection bandwidth, B_L. Increasing the sampling rate beyond this point results in a negligible improvement of the processed data.

Trade-Offs and Conclusions:

It is apparent from the preceeding that the selection of a tracking filter which will meet the demands of the Minitrack System is made on the basis of a compromise between sampling rate, f_s, and acquisition time. For economic reasons, sampling rate should be as low as possible while still maintaining the sampling criteria for processing data. As discussed earlier, increasing the sampling rate beyond B_L does not improve the processed data; therefore, we recognize the necessity for selecting a tracking filter on the basis of bandwidth B_L, since the narrower the bandwidth required to maintain a desired Minitrack resolution, the lower the required sampling rate for processing the data; however, it must be remembered that the smaller the bandwidth, the longer transient errors exist.

As previously shown, a second order tracking filter of 5 Hz or greater and a third order tracking filter of 3 Hz or greater will adequately track steady-state phase errors while maintaining a residual error of .36°. Because of uncertainties involved in attempting acquisition prior to the main lobe null, it is advisable to count on acquiring only after this null point is passed. A 3 Hz third order tracking filter will not perform with this constraint because of the duration of its transient response. Increasing the bandwidth to 20 Hz[5] alleviates the problem but at the expense of added noise and increased sampling rate. A 5 Hz second order tracking filter will provide the necessary tracking accuracy and acquisition time without going to the wider third-order loop and higher sampling frequency.

In view of the above considerations, appropriate values for a tracking filter bandwidth and sampling rate are considered to be 5 Hz and 5 samples per second providing the type of tracking loop utilized is second order.

Acknowledgements:

The authors wish to acknowledge Mr. John Lavery for his programming and computer data gathering efforts and Mr. Tom Grenckik and Mr. Ralph Taylor for their valuable comments and suggestions.

REFERENCES

1. Kruger, B., "Filter Properties of Least Squared Fitted Polynomials," NASA X-551-68-147, January 1968.

2. Simas, V. R., "Signal Level Performance of the Interferometer Re-entry Tracker," X-523-65-199, May 10, 1965.

3. Reedy and Mallinckrodt, "Passive Ranging Doppler System," Report No. 961, Contract DA-04-495-ORD-483, November 2, 1953.

4. Gardner, F. M., "Phaselock Techniques," John Wiley & Sons Inc., N. Y., 1966.

5. Grenckik, T. J. and C. W. Murray, "Minitrack Post Detection Bandwidth Considerations," NASA, GSFC X-557-70-171, June 1970.

6. Kruger, B., "Effects of Corrected Noise with Applications to Apollo Tracking Problems," NASA TN D-4121, February 1968.

BIBLIOGRAPHY

1. Woodman, Ronald F., "A Phase-Locked-Phase-Filter for the Minitrack System," NASA TN D-1418, September 1962.

2. "136 MC Minitrack Interferometer System," Instruction Manual, Volumes 1 and 2, GSFC, NASA.